

Original Article

Implementation of PV-Wind based Microgrid System using Whale Optimization Algorithm

R. K. Negesh¹, S. Karthikeyan², Tharwin Kumar³, M. Sivasubramanian⁴

¹Department of Electrical and Electronics Engineering, Marthandam College of Engineering and Technology, Kuttakuzhi, India

²Department of Electronics and Communication Engineering, KSR College of Engineering, Thiruchengode, India

³Department of Electrical and Electronics Engineering, Puducherry Technological University, Puducherry, India

⁴Department of Electrical and Electronics Engineering, Sri Venkateswara College of Engineering and Technology, Thiruvallur, Tamil Nadu, India

¹Corresponding Author : negeshrk123@gmail.com

Received: 11 January 2023

Revised: 27 March 2023

Accepted: 11 April 2023

Published: 27 April 2023

Abstract - Recently, Micro Grids (MGs) have become extremely popular due to their advantages of effective power conversion and high transmission efficiency. The MG and Nonlinear Loads (NL) are being incorporated into the electricity network. MGs are connected by Voltage Source Converters (VSCs), and NL infuses harmonics into the utility grid using power devices. However, the emergence of stability problems in the MG is caused by the nonlinear characteristics of Renewable Energy Sources (RESs), the rising use of power electronic devices and unexpected variations in load. This paper aims to suggest a microgrid that employs RESs comprising wind and Photovoltaic (PV) systems. This method is established to distribute stable power to loads without any interruptions. A Doubly Fed Induction Generator (DFIG) is deployed as a wind system. To stabilize the PV input voltage, the Boost converter is implemented. Furthermore, intended for enhancing the microgrid's performance, a constant output without distortion is attained from the converter with the deployment of a Whale Optimized Proportional Integral (WO-PI) controller. The 3ϕ inverter is utilized to sustain the DC link voltage, and it combines PV, wind, and battery output at a single point and feeds it to the grid. The results are implemented using the MATLAB platform, and simulation outcomes show that the suggested control technique is effective with a THD of 2.33% and reduced overshoot issues.

Keywords - PV system, Wind system, Boost converter, WO-PI controller, MG, DFIG.

1. Introduction

RESs have recently taken substantial importance as a consequence of the increasing need for electricity. Using innovative, clean energy sources has become essential due to the demand for fossil fuels for power generation [1-3]. As a result, the construction of clean energy using wind and PV input power is projected to be a feasible option in the future. Solar and wind energies are affordable to use and produce no emissions. Also, it brings electricity to isolated locations not handled by electricity companies or connected to the grid. Furthermore, it can provide a remedy for nations experiencing a shortage of fossil fuel energy [4, 5].

Unfortunately, the accessibility of these sources is intermittent and weather-dependent. The power system has challenges while using these resources because of the unpredictable nature of power output and its variations [6]. The utility grid's stability and standalone applications ultimately depend on incorporating clean energy sources [7]. So, adopting Energy Storage Systems (ESS) offers a fantastic

remedy for the intermittent issue. Consequently, hybrid energy systems incorporating ESS are highly suggested to ensure an effective and smooth power transfer. Hence, MGs are a crucial paradigm to combine alongside ESS with distributed and renewable energy sources [9-11].

In the modern world, dealing with the growth of clean energy requires the development of the MG model. It has the potential to enable the final user to store, regulate, produce, and maintain a portion of the energy consumed, turning the client into a contributor to the network instead of a consumer [13]. MG offers numerous benefits to customers and utilities like each other. Reduced power flow on transmission and distribution lines, reduced power losses and lower costs[21,25] for excess energy sources are all benefits of the MG approach. MG can also minimize the load demand on the electrical grid and contributes to lowering pollutants that represent a concern from climate change. Also, it can help in fixing network issues [14].



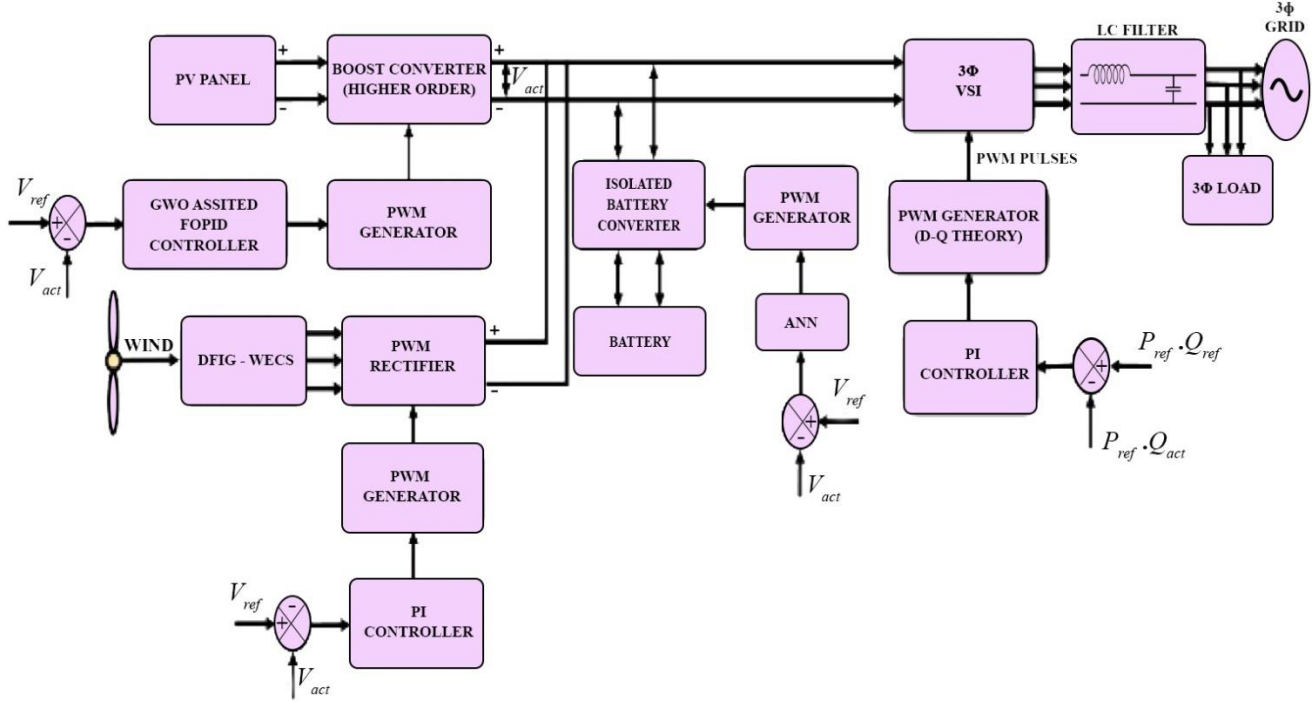


Fig. 1 Schematic diagram for the proposed model

The control strategy's primary goal is to manage the MG's frequency and voltage. Also, it must keep the MG operating steadily while connecting to other networks or dealing with unexpected load variations [15]. The host grid predominately determines the MG frequency and voltage at the common connection point in grid-side mode. As a result, the primary role of the MG control system is to standardize active and reactive power generated by distributed energy resources [16, 18].

Controlling both the PV and wind power generation schemes is essential. An output of PV is a low-voltage DC, which must be converted to a high-voltage DC using DC-DC converters. The following list of DC-DC converters that can be used with PV systems has been reviewed: The most popular converters are Boost converters because they can enhance PV voltage and are appropriate for low-power applications. It also manages the PV voltage and inductor current [19, 20]. In this paper, the Boost converter is suggested for the PV structure, whereas the control of the DFIG-fed wind system is accomplished by a PI controller.

Recent times include employing optimization approaches to improve and regulate the behavior of complex systems. Nonetheless, researchers are quickly and generally utilizing evolutionary optimization for excellent applications. It is regarded as an essential improvement to the PSO algorithm. It benefits from quick convergence, little memory usage for computation, and quick execution [22- 24]. The WO algorithm is a current, effective search method. The whale optimization algorithm (WOA) replicates actions that include shrinking and

enveloping prey, spiral bubble-net attacking prey and variation hunting for prey intending to determine the optimal remedy. It is inspired by the bubble-net assaulting mechanism used by humpback whales.

In contrast to PSO, the WAO has to tune a less number of parameters. In order to optimize difficult issues, it is frequently utilized [26-28]. The PI controller of the nonlinear power system is significantly tuned using the WOA [29, 30].

This paper proposes the PV-Wind-based MG, intended to enhance the power supply during abnormal conditions. The suggested converter provides high efficiency to the system. The parameters are tuned optimally with the assistance of WOA, and it improves the performance of MG in an effective manner. According to the research outcomes, the suggested microgrid can efficiently transfer power to the load without any distortions.

2. Proposed System

As shown in Figure 1, this paper provides a reliable operating approach for a solar and wind hybrid power system-based MG system. Three primary components can be identified: the battery storage systems, PV and wind systems interconnected to the DC-link.

The bidirectional converter is incorporated to provide optimal load management using a dynamical modelling and control system powered by a PV system and wind. Using bidirectional converters, the DC bus is linked to the battery.

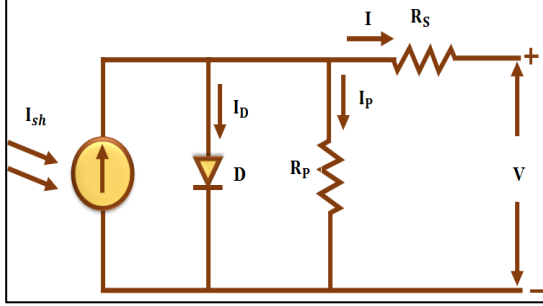


Fig. 2 Equivalent circuit of PV panel

The DFIG technique provides optimal energy extraction from low wind speeds while minimizing mechanical demands on the turbine during wind bursts. It enables small-scale residential-driven operations, maintains gearbox operation and transforms electricity with optimal efficiency. By utilizing the WOA algorithm, the parameters of the PI controller are fine-tuned efficiently. The PI controller with optimization examines the generator's reference speed to determine the maximal power at the speed of the wind turbine. AC and the DC bus are connected to unique AC and DC loads. The battery supplies the load in situations with reduced wind speed or low solar irradiation. Using DC/AC converters, DC bus voltages and battery voltages are connected to AC load requirements. As a result, excess power generated in the system is stored. The detailed explanation of the proposed modelling is explained below.

3. Proposed System Modelling

3.1. Modelling of PV System

In general, solar energy is converted into electrical energy using PV technology. A cell is a single photovoltaic (PV) device. The PV cells are arranged in parallel and in series to create a solar panel. The number of parallels and series cells determines the PV panel's voltage and current. The equivalent circuit model is represented in Figure 2; it is frequently utilized to trigger the properties of PV arrays because they are nonlinear devices.

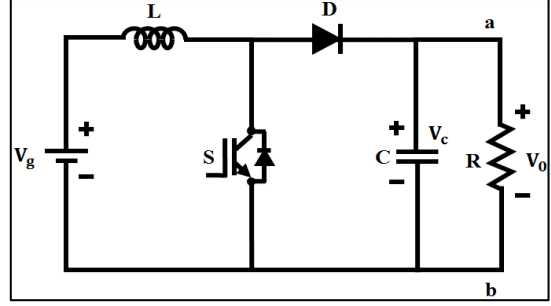
The general equation of the PV panel is given by:

$$I_{pv} = I_{sh} - I_d - I_p \quad (1)$$

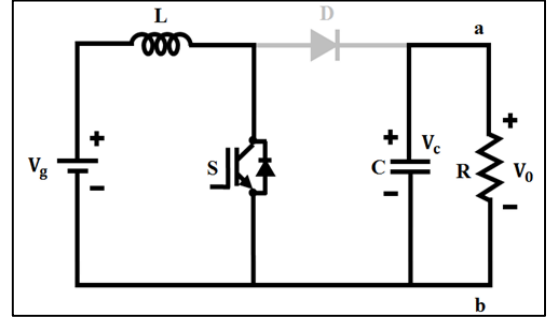
I_d is the current via a diode, and I_p is the current flowing through the circuit's parallel resistance, and they are given in Equations (2) and (3), respectively.

$$I_d = I_o \left[\exp \left(V + \frac{IR_s}{av_T} \right) - 1 \right] \quad (2)$$

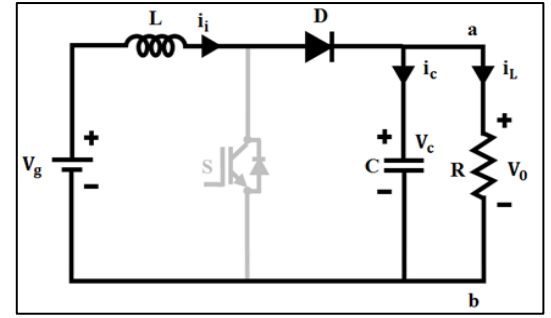
$$I_p = \left(V + \frac{IR_s}{R_p} \right) \quad (3)$$



(a)



(b)



(c)

Fig. 3 (a) Boost converter (b) ON state (c) OFF state

By including Eq. (2) and Eq. (3) in Eq. (1), the attained equation is

$$I_{pv} = I_{sh} - I_o \left[\exp \left(V + \frac{IR_s}{av_T} \right) - 1 \right] - \left(V + \frac{IR_s}{R_p} \right) \quad (4)$$

I-V and P-V curves can be derived from the full, characteristic equation of the PV panel model, Eq. (4), which comprises the independent variables at any test conditions. A suitable converter is utilized to regulate constant output voltage from the PV panel. This work uses a Boost converter that is explained as follows.

3.2. Boost Converter

The PV module generally transforms heat energy into DC voltage by employing a simple Boost converter that permits input currents with minimized distortions. An output of a high voltage level is attained from an input of a low voltage level.

Figure 3 illustrates the schematic diagram for Boost Converter.

The power IGBT is used as a switch in the Boost converter. There are two modes of operation for the circuit. When the IGBT switch is turned ON at $t = 0$, Stage-1 begins. Through L and IGBT switch, the increasing current flows continuously. While the IGBT switch is turned OFF at $t = t1$, stage-2 initiates. The IGBT's current would pass through L , C , the load, and diode D before returning to the IGBT—an inductor current declines until the IGBT switch is turned back on in the following cycle. The energy held in inductor L is transferred to the load. The operation of the converter is further enhanced with the assistance of the PI controller, and this paper employs WOA to adjust the parameters of the PI controller.

3.3. Whale Optimized PI Controller (WO-PI)

3.3.1. PI Controller

A PI controller is an established controller capable of maintaining accurate set points. The functional modelling of the PI controller is based on a combination of two control modes, proportional and integral. The PI controller is gained from k_p and k_i parameters by using logical expression. Equation (10) declares the general form of PI controller where k_p is the proportional gain and k_i is the integral gain.

$$u(t) = k_p e(t) + k_i \int e(t) dt \quad (5)$$

Using the Laplace transform, equation (11) is changed to equation (12)

$$U(s) = k_p E(s) + \frac{k_i E(s)}{s} \quad (6)$$

Equation (11) is the expression of PI with respect to the time constraint.

$$U(s) = k_p [1 + \frac{1}{\tau_i}] E(s) \quad (7)$$

Where $k_i = \frac{k_p}{\tau_i}$ and $k_p = k_d / \tau_i$

For a closed-loop control system, when precise tuning of k_p and k_i values are performed, then there is a small decrease in the rise time and improvement in the proposed system. Compared to several software-based concepts realized to aid in controller tuning, the proposed optimization for the PI controller has recently been implemented to improve control performance.

3.3.2. Whale Optimization Algorithm

The manoeuvre is performed by humpback whales that plunge to deep levels, surround their prey with bubbles in a spiral pattern, and then swim to the top. Usually, they go after

the little fishes swimming near the surface. A mathematical representation of the WOA describes the actions of encircling the prey, setting up spiral bubbles manoeuvres, and searching for the prey. Modeling of the algorithm is explained as follows:

Encircling the Prey:

WOA examines the prey position as a feasible conclusion. These equations can be used to model when humpback whales surround their prey.

$$D = |C \cdot X_p(t) - X(t)| \quad (8)$$

$$X(t + 1) = X_p(t) - A \cdot D \quad (9)$$

Where t is the current iteration, $X_p(t)$ is the position vector of the prey, $X(t)$ is the whale's position vector, and A and C are coefficient vectors.

$$A = 2a \cdot r - a \quad (10)$$

$$C = 2 \cdot r \quad (11)$$

With consistent iteration, the vector a decreases linearly from 2 to 0 while the random vector r fluctuates between 0 and 1.

Bubble Attacking of the Prey:

The attacking procedure emphasizes the WOA's exploitation or local search. There are two ways to explain how whales behave when assaulting their prey by blowing bubbles. The following is a mathematical model of a whale's behavior:

Shrinking Encircling Mechanism:

In this technique, a whale swims through every circle around their prey. This can be done by iteratively decreasing a from 2 to 0 and fixing $|A| < 1$.

Spiral Updating Position:

Humpback whales perform a spiral-shaped manoeuvre as they approach their prey. To update the whale's location, the below equations are utilized:

$$X(t + 1) = D' \cdot e^{bl} \cdot \cos(2\pi l) + X_p(t) \quad (12)$$

$$D' = |X_p(t) - X(t)| \quad (13)$$

Where l is a random number that occurs in the middle of -1 and 1, and b is a constant that specifies a spiral logarithmic shape. During the attack, whales display two strategies concurrently. As a result, it is expected that the spiral model and the shrinking encircling mechanism are expected to update their positions, which can be depicted as follows.

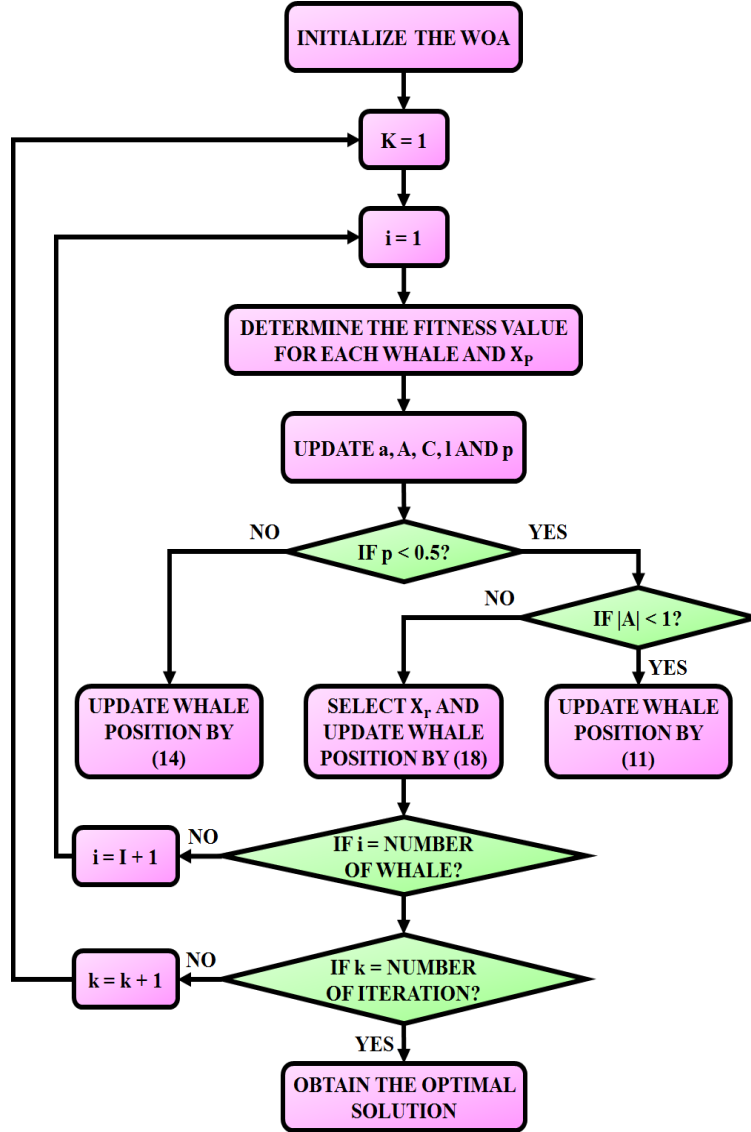


Fig. 4 Flowchart of WOA

$$X(t + 1) = \begin{cases} X_p(t) - A \cdot D & \text{if } p < 0.5 \\ D' \cdot e^{bl} \cdot \cos(2\pi l) + X_p(t) & \text{if } p \geq 0.5 \end{cases} \quad (14)$$

Searching for the Prey:

The WOA conducts its exploration or worldwide search throughout this process as the humpback whales look for prey. It is discovered that the search process can be expressed by $|A| > 1$. The position of the whales or an agent can be updated as follows:

$$D = |C \cdot X_p(t) - X(t)| \quad (15)$$

$$X(t + 1) = X_p(t) - A \cdot D \quad (16)$$

Where, $X_p(t)$ is a random vector of whale position.

In Figure 4, the WOA model is illustrated. It begins with a random population of humpback whales in the search area and ends with X_p . With the assistance of WOA, the parameters of the PI controller are tuned efficiently. The proposed control approach results in improved characteristics like minimized peak overshoot issues with reduced settling time, thereby aiding in enhanced control performance.

3.4. Wind Turbine (WT) Modelling

It is common for solar panels to be highly resistant to wind damage. However, during the summertime, solar panels gather solar energy, but in winter conditions, the PV system cannot accomplish this in cloudy conditions. In order to generate power in these circumstances, an alternating wind turbine source is used. According to the consecutive expression, wind speed affects the amount of electricity the WT generates.

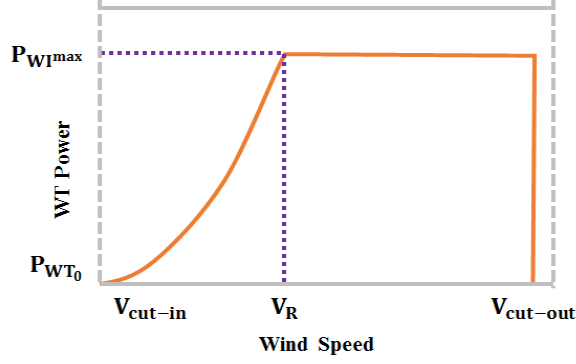


Fig. 5 Wind speed with a variation of WT power

$$P_{WT}(t) = \begin{cases} 0, & V < V_{cut-in} \text{ or } V < V_{cut-out} \\ P_{WT}^{max} \left(\frac{P_{WT0} - P_{WT}^{max}}{V_{cut-out} - V_R} \right) (V(t) - V_R), & V_{cut-in} \leq V \leq V_R \\ P_{WT}^{max} \left(\frac{V(t) - V_{cut-in}}{V_R - V_{cut-in}} \right)^3, & V_R < V \leq V_{cut-out} \end{cases} \quad (17)$$

Where P_{WT}^{max} the maximum power of the WT is, $V_{cut-out}$ is cut-out speed, V_R is the nominal speed of the wind and V_{cut-in} is cut-in speed, $V(t)$ is the instant speed of the wind and P_{WT0} is the power of the WT at $V_{cut-out}$. Following is an expression of the power produced by N_{WT} WT at instant t .

$$P_{WT}(t) = N_{WT} \times P_{WT}(t) \quad (18)$$

Efficient power management is provided by the proposed work with the inclusion of a battery source. In order to store the excess electrical power from the PV-wind system, the battery is deployed here.

3.5. Modelling of Battery

In cases where the electricity produced by the deployed RESs is insufficient, a battery assists in providing the load. According to the necessary demand, the battery capacity is shown as follows:

$$C_{Bat} = AD \times \frac{P_L}{\eta_{Inv} \eta_{Bat} DOD} \quad (19)$$

Where P_L is demand power, η_{Bat} is battery efficiency, η_{Inv} is the efficiency of the inverter, DOD is the battery depth of discharge. RESs are used as a source of backup power when the generated power exceeds the amount needed to charge the battery. As a result, the battery power is determined as shown in:

$$C_{Batt} = P_{PV}(t) + P_{WT}(t) - \frac{P_L(t)}{\eta_{Inv}} \quad (20)$$

State of Charge ($SOC(t)$), predicated on the amount of excess or shortage of RESs power produced over demand, is a crucial consideration impacting battery efficiency. It can be displayed as follows.

$$\begin{cases} SOC(t-1)(1-\delta) + \left((P_{PV}(t) + P_{WT}(t)) - \frac{P_L(t)}{\eta_{Inv}} \right) \times \eta_{Bat}, & (P_{PV}(t) + P_{WT}(t)) > P_L(t) \\ SOC(t-1)(1-\delta) + \left(\frac{P_L(t)}{\eta_{Inv}} - (P_{PV}(t) + P_{WT}(t)) \right) \eta_{Bat}, & (P_{PV}(t) + P_{WT}(t)) < P_L(t) \end{cases} \quad (21)$$

Where, δ is the self-discharge rate of the battery. The battery, along with the solar and wind sources, provides enhanced energy management, thereby preventing the conditions of power shortages.

3.6. Three-Phase Grid Synchronization

This paper examines the control techniques for grid-connected VSIs. Consequently, for the current controller to prevent harmonics, it provides a high-quality sinusoidal output with little distortion to influence how the inverter supplies current to the grid. PI controllers with grid voltage paths are utilized for inverter control. In a synchronous reference frame, an active (P) and reactive power (Q) delivered to the grid can be stated as

$$P = 1.5(Vod id + Voq iq) \quad (22)$$

$$Q = 1.5(Vod iq + Voq id) \quad (23)$$

Where the Vod, Voq, id, iq are the voltages and currents after the filter in dqo reference frame and P, Q are the active and reactive power respectively. Since that Voq is assumed to be zero, (22) and (23) can be expressed as

$$P = 1.5(Vod id) \quad (24)$$

$$Q = 1.5(Vod iq) \quad (25)$$

id and iq can be derived from the aforementioned equations as follows:

$$id = 2p/3Vod \quad (26)$$

$$iq = 2p/3Vod \quad (27)$$

With the help of 3 ϕ grid synchronization, the power is delivered to the load without any distortions, and the enhanced power flows continuously to the grid. Thus the proposed work contributes uninterrupted power supply along with enhanced dynamic outputs.

4. Results and Discussion

An efficient optimization algorithm for a PV-wind-based MG system using a Boost converter is analyzed in this paper. The obtained outcomes of the suggested work are validated, and the comparable waveforms are illustrated. Figure 6 denotes that the variation in temperature at 0.2s impacts the current and voltage of the solar panel. From the waveform, it is identified that the voltage increases from 175V to 180 V, and the current increases to 41 A; after that, it maintains the constant value of 3A from 0.01s.

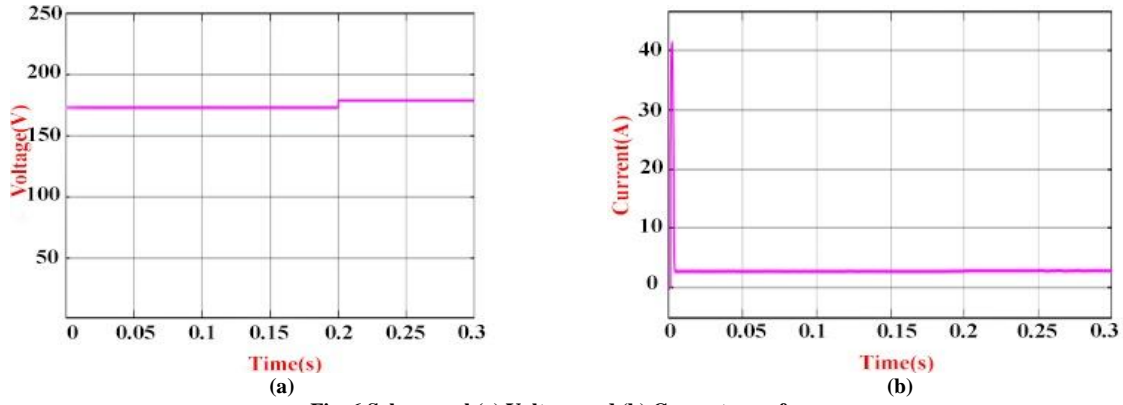


Fig. 6 Solar panel (a) Voltage and (b) Current waveform

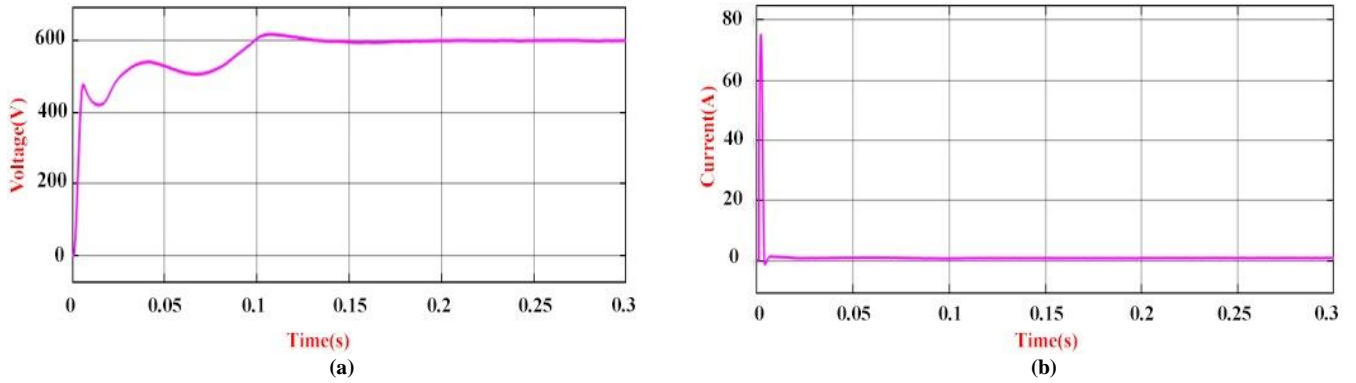


Fig. 7 Output (a) Voltage and (b) Current waveform of the boost converter

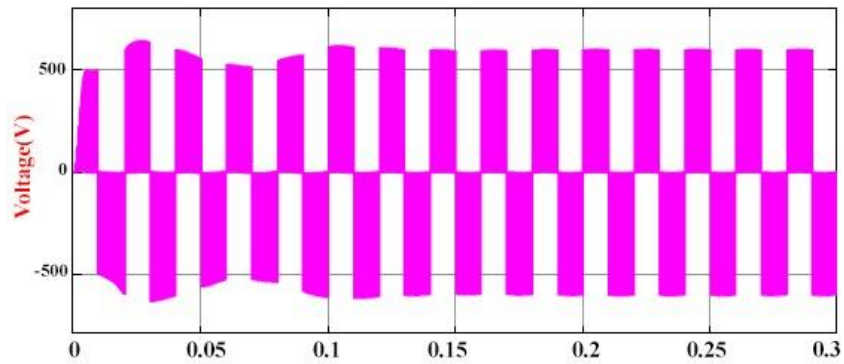


Fig. 8 Output voltage of DFIG at WT side

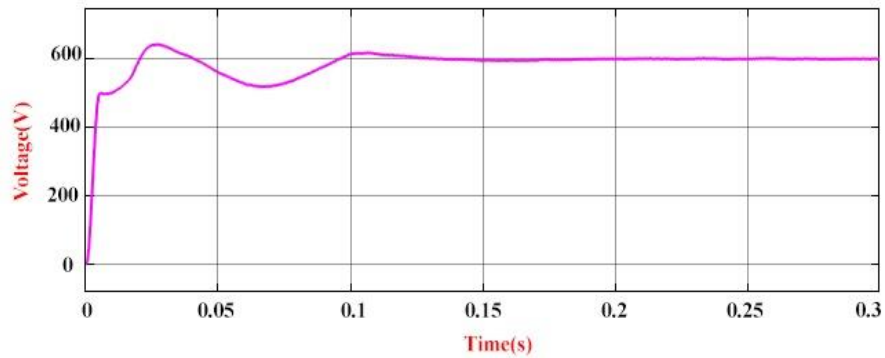


Fig. 9 PWM rectifier output

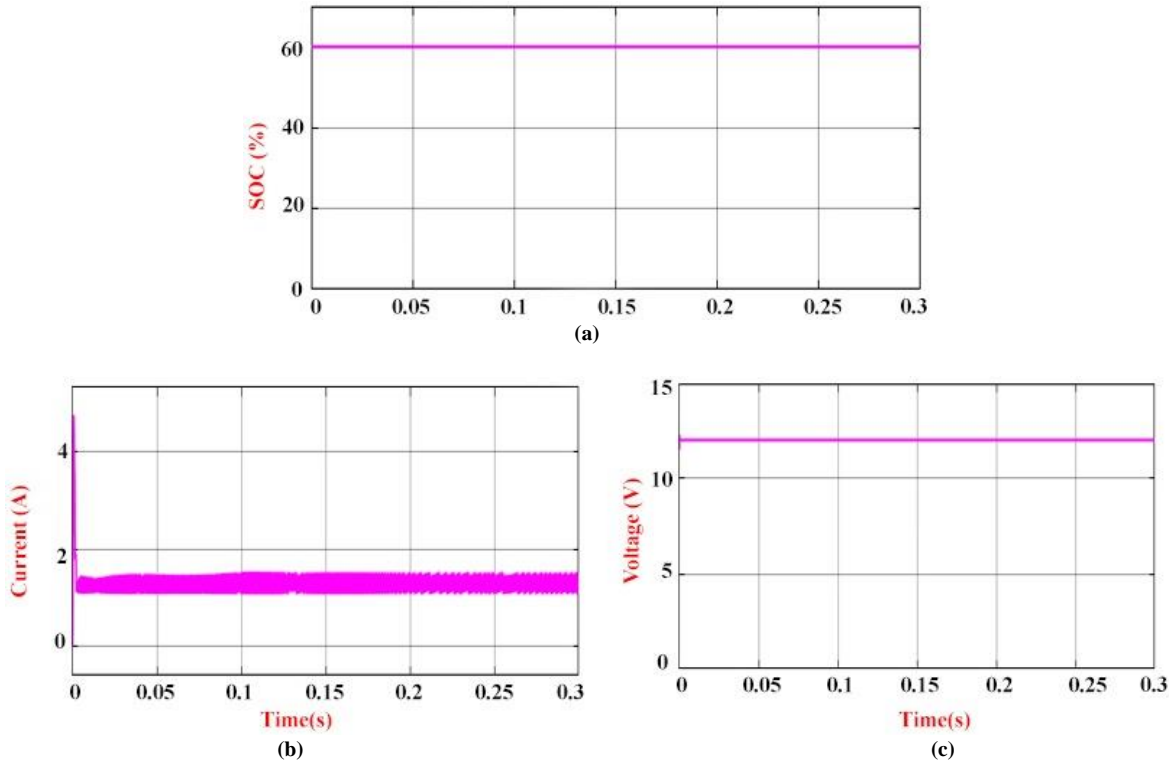


Fig. 10 Battery (a) SOC (b) Current (c) Voltage waveform

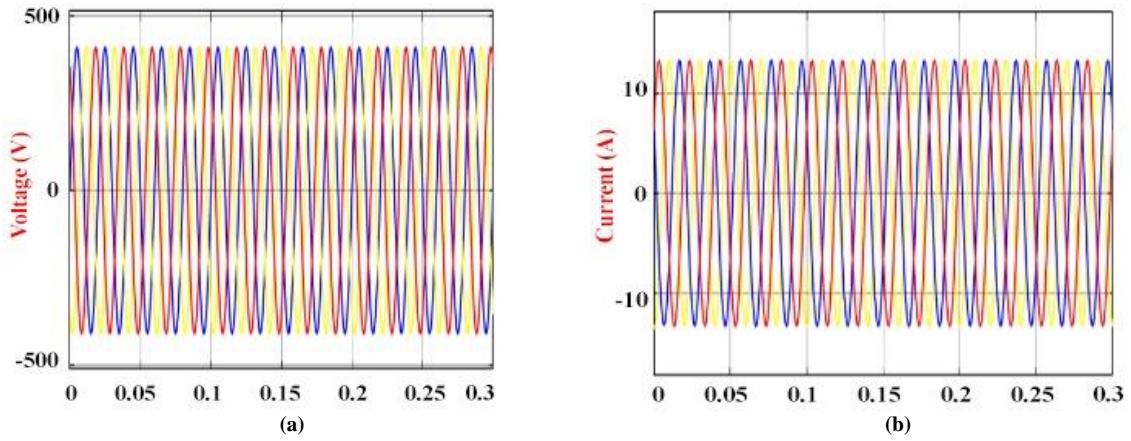


Fig. 11 Grid (a) Voltage and (b) Current

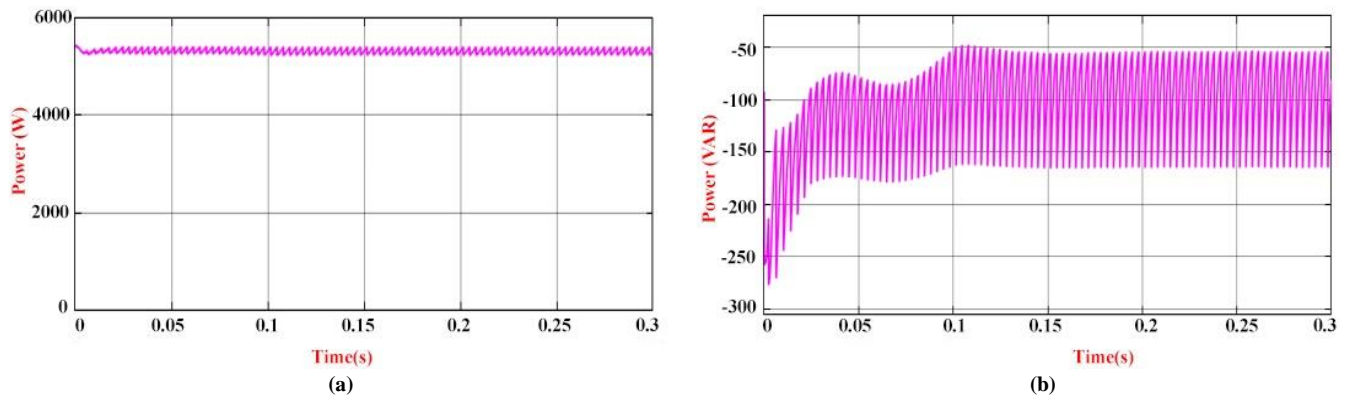


Fig. 12 Real and reactive power waveform

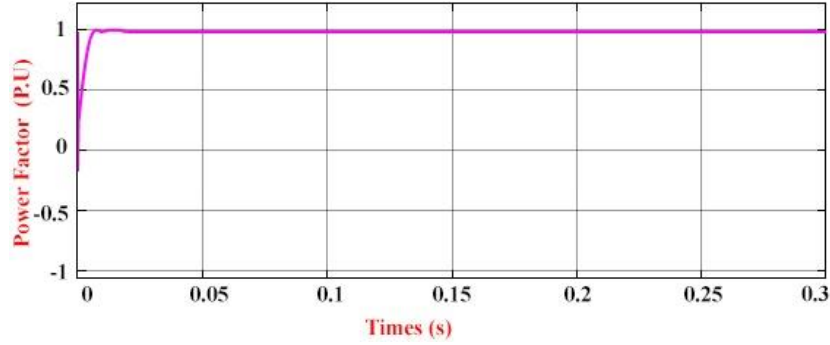


Fig. 13 Waveform of power factor

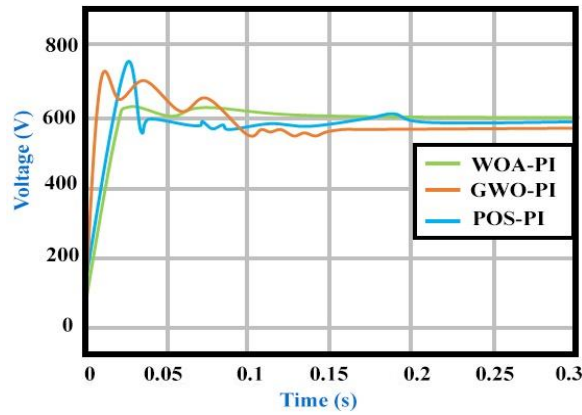


Fig. 14 Transient response of WOA compared with GWO and PSO approach

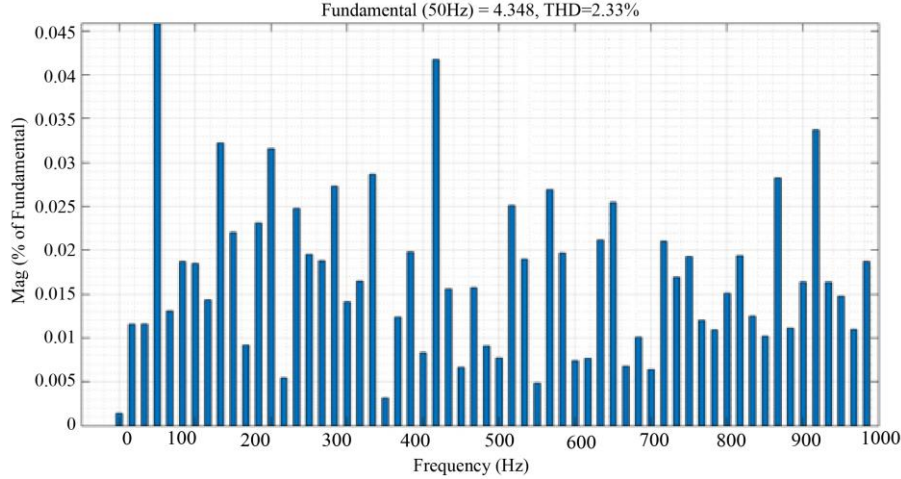


Fig. 15 THD value

The parameter specifications are given in the Table 1. The Boost converter's output voltage and current waveforms are represented in Figure 7. After certain variations, the converter output voltage of 600V is accomplished at 0.15 sec. Likewise, the output converter current is maintained the constant value of 1A at 0.01 sec. Despite the fluctuations of PV inputs, the converter generates a controlled output with the optimized control.

Figure 8 demonstrates the DFIG-based output voltage of the suggested system. Here the voltage value obtained is 600 V. Similarly, the PWM rectifier output is shown in Figure 9, where the voltage is maintained at around 600 V.

Figure 10(a) illustrates the graph representation for the battery system; here, the state of charge obtained is 60%, and 10(b) represents that a current of 1.5A is maintained, 10(b) shows that a constant voltage of 12V is maintained in the battery.

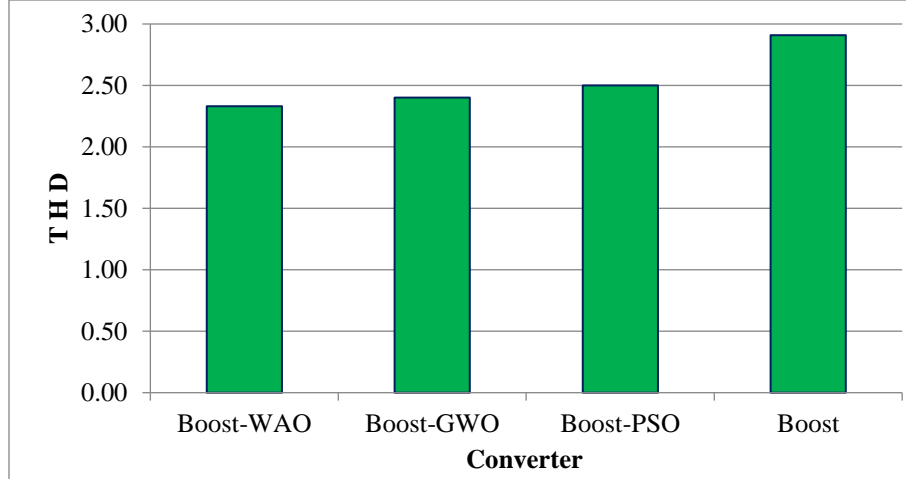


Fig. 16 Comparison analysis

Table 1. Parameter specifications

Parameters	Ratings
Solar panel	
Peak power	10kW
No. of Panels	20 panels
Short circuit voltage	12V
Open circuit voltage	22.6V
Series connected solar PV cells	36
WECS	
No. of Turbines	1
Power	10kW
Voltage	575V
Boost Converter	
C	190μF
L	380βH
R _L	50ohms

The above waveforms in Figure 11 represent the grid voltage and current; from the observations, it is clear that a constant voltage of 430V and 15 A is given to the grid. The stable current value of 14 A is attained.

In contrast to real and reactive power, the 3ϕ grid synchronization is accomplished. Figure 12 indicates the

waveforms for real and reactive power for 3ϕ grid. Here, the real power is maintained stable at 5200W at 0.1 sec, and a reduced reactive power is obtained.

Figure 13 illustrates the power factor waveform. Here, a power factor of 0.989 is obtained, which indicates the efficient functioning of the proposed system with reliable power.

Maximum overshoot, settling time and rise time specifications for WOA employing PI are shown in Table 2. Also, using a PI controller, this table compares WOA with other optimization approaches like GWO and PSO. According to the table, WOA has the smallest maximum overshoot and settling time, indicating a quicker response time but a slower rise time than the other systems. Figure 14 displays the transient response for all optimization techniques.

Figure 15 displays the suggested converter's THD value as 2.33% with minimized harmonics. Moreover, the continuous power flow is established without any interruptions.

Table 3 denotes that the comparative analysis of THD value with different approaches and corresponding plots are represented in Figure 16. The proposed Boost-WOA attains a low THD value of 2.33%. It gives a better result compared to other techniques.

Table 2. Requirements for transient responses to various optimization

Optimization	K _p	K _i	Max Over shoot (s)	Rise Time (s)	Settling time (s)
WOA-PI	0.7843	0.9962	0.025	0.02	0.14
GWO-PI	0.9564	0.9934	0.015	0.01	0.17
PSO-PI	1.773	0.3672	0.025	0.02	0.22

Table 3. Comparison analysis

CONVERTER	THD
Boost-WAO	2.33%
Boost-GWO	2.40%
Boost-PSO	2.50%
Boost	2.91%

5. Conclusion

Currently, the RES is being employed increasingly to facilitate and fulfil the enhanced energy demands resulting from economic development and population explosion. The MG is grid-connected. The reliable operation enforces common bus conditions (voltage and frequency) and organizes any imbalance between generation and

consumption. In this paper, the suggested approach efficiently manages the switching between the wind turbine and battery storage system while obtaining more power from the PV panel. Here, intending to separate the excess power from WT, the DFIG is used. Depending on an optimization process, the established technique assists in attaining the system's overall expenses while assuring a quite reliable source of load power. The designed PI controller involves ensuring smooth power output. By utilizing the whale-optimized PI controller, the constant output voltage is attained successfully without interruptions. The attained outcomes show that the proposed method is efficient compared to other control approaches with a reduced THD of 2.33%.

References

- [1] Muhammad Fahad Zia et al, "Energy Management System for A Hybrid Pv-Wind-Tidal-Battery-Based Islanded Dc Microgrid: Modeling and Experimental Validation," *Renewable and Sustainable Energy Reviews* vol. 159, pp. 112093, 2022. [[CrossRef](#)] [[Google Scholar](#)] [[Publisher Link](#)]
- [2] Ujjwal Datta, Akhtar Kalam, and Juan Shi, "Hybrid Pv-Wind Renewable Energy Sources for Microgrid Application: An Overview," *Hybrid-Renewable Energy Systems in Microgrids*, pp. 1-22, 2018. [[CrossRef](#)] [[Google Scholar](#)] [[Publisher Link](#)]
- [3] Shakti Singh, Mukesh Singh, and Subhash Chandra Kaushik, "Feasibility Study of An Islanded Microgrid in Rural Area Consisting of PV, Wind, Biomass and Battery Energy Storage System," *Energy Conversion and Management*, vol. 128, pp. 178-190, 2016. [[CrossRef](#)] [[Google Scholar](#)] [[Publisher Link](#)]
- [4] Cameron Smith et al., "Comparative Life Cycle Assessment of a Thai Island's Diesel/Pv/Wind Hybrid Microgrid," *Renewable Energy*, vol. 80, pp. 85-100, 2015. [[CrossRef](#)] [[Google Scholar](#)] [[Publisher Link](#)]
- [5] Wanxing Sheng et al., "Research and Practice on Typical Modes and Optimal Allocation Method for Pv-Wind-Es in Microgrid," *Electric Power Systems Research*, vol. 120, pp. 242-255, 2015. [[CrossRef](#)] [[Google Scholar](#)] [[Publisher Link](#)]
- [6] Ayman Al-Quraan, and Muhannad Al-Qaisi, "Modelling, Design and Control of a Standalone Hybrid Pv-Wind Micro-Grid System," *Energies*, vol. 14, pp. 4849, 2021. [[CrossRef](#)] [[Google Scholar](#)] [[Publisher Link](#)]
- [7] Tathagata Sarkar et al., "Optimal Design and Implementation of Solar PV-Wind-Biogas-VRFB Storage Integrated Smart Hybrid Microgrid for Ensuring Zero Loss of Power Supply Probability," *Energy Conversion and Management*, vol. 191, pp. 102-118, 2019. [[CrossRef](#)] [[Google Scholar](#)] [[Publisher Link](#)]
- [8] S.Priyanka et al., "Iot Based Hybrid Artificial Tree for Solar/Wind Power Generation With Pollution Control and Monitoring," *SSRG International Journal of Computer Science and Engineering*, vol. 8, no. 4, pp. 1-3, 2021. [[CrossRef](#)] [[Publisher Link](#)]
- [9] Rajvikram Madurai Elavarasan et al., "Investigations on Performance Enhancement Measures of the Bidirectional Converter in Pv-Wind Interconnected Microgrid System," *Energies*, vol. 12, no. 14, pp. 2672, 2019. [[CrossRef](#)] [[Google Scholar](#)] [[Publisher Link](#)]
- [10] Boualam Benlahbib et al., "Experimental Investigation of Power Management and Control of a Pv/Wind/Fuel Cell/Battery Hybrid Energy System Microgrid," *International Journal of Hydrogen Energy*, vol. 45, no. 53, pp. 29110-29122, 2020. [[CrossRef](#)] [[Google Scholar](#)] [[Publisher Link](#)]
- [11] Makbul A.M. Ramli, H.R.E.H. Bouchekara, and Abdulsalam S. Alghamdi, "Optimal Sizing of Pv/Wind/Diesel Hybrid Microgrid System Using Multi-Objective Self-Adaptive Differential Evolution Algorithm," *Renewable Energy*, vol. 121, pp. 400-411, 2018. [[CrossRef](#)] [[Google Scholar](#)] [[Publisher Link](#)]
- [12] Ahmad Al-Sarraj et al., "Simulation Design of Hybrid System (Grid/Pv/Wind Turbine/ Battery /Diesel) with Applying Homer: A Case Study in Baghdad, Iraq," *SSRG International Journal of Electronics and Communication Engineering*, vol. 7, no. 5, pp. 10-18, 2020. [[CrossRef](#)] [[Google Scholar](#)] [[Publisher Link](#)]
- [13] Tamer Khatib, Azah Mohamed, and K. Sopian, "Optimization of a Pv/Wind Micro-Grid for Rural Housing Electrification Using a Hybrid Iterative/Genetic Algorithm: Case Study of Kuala Terengganu, Malaysia," *Energy and Buildings*, vol. 47, pp. 321-331, 2012. [[CrossRef](#)] [[Google Scholar](#)] [[Publisher Link](#)]
- [14] A. AlKassem, M. Al Ahmadi, and A. Draou, "Modeling and Simulation Analysis of A Hybrid Pv-Wind Renewable Energy Sources for A Micro-Grid Application," *2021 9th International Conference on Smart Grid Icsmartgrid*, *IEEE*, pp. 103-106, 2021. [[CrossRef](#)] [[Google Scholar](#)] [[Publisher Link](#)]
- [15] Zakria Qadir et al., "Predicting the Energy Output of Hybrid Pv-Wind Renewable Energy System Using Feature Selection Technique for Smart Grids," *Energy Reports*, vol. 7, pp. 8465-8475, 2021. [[CrossRef](#)] [[Google Scholar](#)] [[Publisher Link](#)]

- [16] Ahmed Fathy, Khaled Kaaniche, and Turki M. Alanazi, "Recent Approach Based Social Spider Optimizer for Optimal Sizing of Hybrid Pv/Wind/Battery/Diesel Integrated Microgrid in Aljouf Region," *IEEE Access*, vol. 8, pp. 57630-57645, 2020. [[CrossRef](#)] [[Google Scholar](#)] [[Publisher Link](#)]
- [17] Harshal D. Vaidya, Dr. S. M. Badave, and Ruchita P. Dahad, "Hardware Implementation of Non-Isolated Sextuple Output Hybrid Converter," *International Journal of Engineering Trends and Technology*, vol. 67, no. 11, pp. 174-183, 2019. [[CrossRef](#)] [[Google Scholar](#)] [[Publisher Link](#)]
- [18] Linus A. Alwal, Peter K. Kihato, and Stanley I. Kamau, "A Review of Control Strategies for Microgrid with Pv-Wind Hybrid Generation Systems," *Proceedings of the Sustainable Research and Innovation Conference*, 2022. [[Google Scholar](#)] [[Publisher Link](#)]
- [19] Yinghao Shan et al., "Model Predictive Control of Bidirectional Dc–Dc Converters and Ac/Dc Interlinking Converters—A New Control Method for Pv-Wind-Battery Microgrids," *IEEE Transactions on Sustainable Energy*, vol. 10, no. 4, pp. 1823-1833, 2018. [[CrossRef](#)] [[Google Scholar](#)] [[Publisher Link](#)]
- [20] R. Rajasekaran, and P. Usha Rani, "Bidirectional Dc-Dc Converter for Microgrid in Energy Management System," *International Journal of Electronics*, vol. 108, no. 2, pp. 322-343, 2021. [[CrossRef](#)] [[Google Scholar](#)] [[Publisher Link](#)]
- [21] Edgar Apaza Huallpa et al., "Low Power and Cost-Optimized Equipment Design for the Measurement of Resistivity in Austenitic Steels," *International Journal of Engineering Trends and Technology*, vol. 69, no. 10, pp. 15-19, 2021. [[CrossRef](#)] [[Publisher Link](#)]
- [22] Mohammed Kharrich, Mohamed Akherraz, and Yassine Sayouti, "Optimal Sizing and Cost of a Microgrid Based in PV, Wind and Bess for a School of Engineering," *2017 International Conference on Wireless Technologies, Embedded and Intelligent Systems Wits*, *IEEE*, pp. 1-5, 2017. [[CrossRef](#)] [[Google Scholar](#)] [[Publisher Link](#)]
- [23] Raja Mouachi et al., "Multiobjective Sizing of an Autonomous Hybrid Microgrid Using a Multimodal Delayed PSO Algorithm: A Case Study of a Fishing Village," *Computational Intelligence and Neuroscience*, 2020. [[CrossRef](#)] [[Google Scholar](#)] [[Publisher Link](#)]
- [24] Ali Dali et al., "Development of a Sizing Interface for Photovoltaic-Wind Microgrid Based on Pso-Lpsp Optimization Strategy," *2018 International Conference on Wind Energy and Applications in Algeria Icwaaa*, *IEEE*, pp. 1-5, 2018. [[CrossRef](#)] [[Google Scholar](#)] [[Publisher Link](#)]
- [25] Phanom Tawdee et al., "Effects of Voltage Gain and Power Losses in Z Source Converter Circuit Using Zero Voltage Switch," *International Journal of Engineering Trends and Technology*, vol. 70, no. 8, pp. 126-131, 2022. [[CrossRef](#)] [[Publisher Link](#)]
- [26] Ahmed A. Zaki Diab et al., "Application of Different Optimization Algorithms for Optimal Sizing of Pv/Wind/Diesel/Battery Storage Stand-Alone Hybrid Microgrid," *IEEE Access*, vol. 7, pp. 119223-119245, 2019. [[CrossRef](#)] [[Google Scholar](#)] [[Publisher Link](#)]
- [27] M Durairasan, and Divya Balasubramanian, "An Efficient Control Strategy for Optimal Power Flow Management From a Renewable Energy Source to A Generalized Three-Phase Microgrid System: A Hybrid Squirrel Search Algorithm with Whale Optimization Algorithm Approach," *Transactions of the Institute of Measurement and Control*, vol. 42, no. 11, pp. 1960-1976, 2020. [[CrossRef](#)] [[Google Scholar](#)] [[Publisher Link](#)]
- [28] Muhammad Hamza Zafar, Noman Mujeeb Khan, and Umer Amir Khan, "Short Term Hybrid Pv/Wind Power Forecasting for Smart Grid Application using Feed Forward Neural Network (FNN) Trained by a Novel Atomic Orbital Search (AOS) Optimization Algorithm," *2021 International Conference on Frontiers of Information Technology Fit*, *IEEE*, pp. 72-77, 2021. [[CrossRef](#)] [[Google Scholar](#)] [[Publisher Link](#)]
- [29] Sajid Hussain Qazi, M.A Uqaili, and U Sultana, "Whales Optimization Algorithm Based Enhanced Power Controller for an Autonomous Microgrid System," *2019 8th International Conference on Modern Power Systems MPS*, *IEEE*, pp. 1-7, 2019. [[CrossRef](#)] [[Google Scholar](#)] [[Publisher Link](#)]
- [30] H.S. Ramadan, "Optimal Fractional Order Pi Control Applicability for Enhanced Dynamic Behavior of on-Grid Solar Pv Systems," *International Journal of Hydrogen Energy*, vol. 42, no. 7, pp. 4017-4031, 2017. [[CrossRef](#)] [[Google Scholar](#)] [[Publisher Link](#)]